

# Improving the reliability of sand-steel interface friction angle measurements based on the Ring Shear test

Abdalla Almukashfi<sup>#</sup>, Svend Pilgaard Larsen, and Nataša Katić

*Geo, Copenhagen, Denmark*

*<sup>#</sup>Corresponding author: abd@geo.dk*

## ABSTRACT

Understanding the shearing behaviour at soil-structure interfaces is crucial for the analysis and design of geotechnical structures. When significant relative displacements between soil and interface are involved during installation or operation, the ring shear interface testing method, which includes large pre-shearing, is considered reliable for assessing interface resistance. These tests are commonly applied in practical design approaches for driven piles. This research aimed to expand the unified database created by Imperial College London (ICL) and Norwegian Geotechnical Institute (NGI) by incorporating soil test data collected by Geo for North Sea sands with varying grain size distributions.

We present an extended database that encompasses soil classification tests and Ring Shear (RS) tests conducted on soil-steel interfaces using Advanced Ring Shear apparatus (Bishop-apparatus-like). This paper introduces a database of interface shearing tests conducted on sandy silty soils with a low content of non-plastic fines. These results facilitate a comprehensive examination of the potential impacts of various factors, including physical soil properties (e.g. grain size distribution), interface characteristics (surface roughness), and testing conditions (normal effective stress). Trends identified within the datasets are synthesized with insights from prior studies to propose interface shear strength parameters suitable for preliminary design employing simple index tests for non-plastic sandy soils. Finally, the paper presents a newly advanced Ring Shear apparatus designed by Wille Geotechnik capable of accommodating static friction. This apparatus incorporates two novel test inserts that can rotate independently at varying radial speeds while being guided simultaneously. The two guided rings can be vertically adjusted, thereby mitigating static friction effects, even in cases of dilatancy.

**Keywords:** Driven piles; advanced ring shear; interface friction angle; shear rate.

## 1. Introduction

The thorough examination and design of diverse offshore and onshore geotechnical structures, like piles, suction buckets, pipelines, shallow foundations, and retaining structures, require a meticulous understanding of soil-structure interface shearing behaviour and careful selection of design parameters. Shear resistance at the soil-pile shaft interface significantly affects the axial capacity of driven piles, demanding precise determination of interface shearing parameters. Interface shearing also affects the analysis of laterally loaded caissons and monopiles, influenced by both shaft and base shear resistances (Andersen et al., 2013). Soil-interface shearing angles ( $\delta'$ ) and dilatancy properties are typically evaluated through various laboratory tests, including direct shear, simple shear, torsional shear, and tests in specialized apparatuses like the ring shear apparatus (Bishop or Bromhead). Jardine et al. (1992) conducted direct shear interface shear tests on a broad range of silica sands shearing above steel interfaces with the average roughness ( $R_a$ ) of typical industrial piles. Later, Jardine & Chow (1996) incorporated a simplified illustrative relationship between interface friction angle and median grain diameter,  $D_{50}$ , into their design guidelines. However, a review by CUR (2001) challenged the validity of this relationship, asserting that

significant displacement during pile driving alters both the particle sizes of granular soils in contact with pile shafts and the surface roughness of the pile itself. As a result, CUR recommended adopting  $\delta' = 29^\circ$  for silica sands regardless of the initial grain size or initial interface condition.

Ring shear tests demonstrate a closer resemblance to the large-displacement conditions adjacent to a driven pile shaft compared to other laboratory tests. According to Coop et al. (2004), particle breakage persists even after significant shear displacements and ceases only upon achieving a stable grain size distribution. Considering these observations, along with arguments presented by CUR (2001), many researchers including Jardine et al. (2005), Ho et al. (2011) and Liu et al. (2019) proposed transitioning to site-specific ring shear tests for assessing pile shaft friction in sands. This transition involves adopting appropriate stress levels, interface materials, and roughness. The Bishop apparatus is particularly useful for interface shear testing, enabling extensive shear displacements, uniform interface shear stress application, and direct measurement of side friction. Preconditioning stages can simulate practical scenarios such as pile installation. In general, the Bishop apparatus is less sensitive to the presence of coarser soil particles because it shears a larger volume of soil using a thicker sample compared to the Bromhead setup. The ring in Bishop setup has inner diameter  $D_i$  of 100mm, outer

diameter  $D_o$  of 150 mm and the sample height  $H$  in this setup is 10 mm. In Bromhead setup, the inner diameter is  $D_i$  is 70mm, the outer diameter  $D_o$  is 100 mm, and the sample height is  $H = 20$  mm. Tests carried out in the Bromhead apparatus typically utilize an upper interface configuration, while those in the more intricate Bishop et al. (1971) equipment generally employ an inverted 'lower inter-face' setup. This selection could influence results, as fine crushed particles might gravitate away from the top interface in upper interface tests instead of being confined within an accumulating basal shear zone as in lower interface experiments. Several researchers show that the Bromhead setup yields better results when used in clayey soil. For instance, Bromhead & Dixon (1986) show broad agreement between somewhat scattered data sets obtained in soil-soil tests on London Clay, while Fearon (1998) also shows generally good agreement in tests on plastic Italian clays. Furthermore, Stark & Eid (1992) have shown that the drained residual strengths measured using a ring shear apparatus on remoulded claystone specimens are in excellent agreement with back analyses of landslides.

This paper presents an extension to the unified database created by ICL and NGI of ring shear interface tests conducted on sandy-silty soils with low percentages of non-plastic fines. These tests, conducted in accordance with ICP procedures, Jardine et al. (2005), are aimed at determining interface friction angles to evaluate axial pile capacity. The dataset, augmented by previous experiments, facilitates an evaluation of the impact of soil properties, interface materials, and surface attributes on interface shear resistance, assisting in the selection of parameters for initial designs. The paper underscores project-specific testing as the most dependable approach for obtaining representative soil-interface shearing angles ( $\delta'$ ) parameters for detailed design purposes. In addition, the paper presents evidence that the Advanced ring shear apparatus (Bishop-like), used in this study, is capable of an accurate estimation of interface friction angle. The following sections present a brief description of the ring shear apparatus and its capabilities, test procedure, test results and the interpretations.

## 2. Material and Method

Advanced ring shear tests were conducted on various sand and sand till samples, with shearing occurring against roughened steel annular interfaces. The complex geology of the materials and the detailed testing procedures are explained below.

### 2.1. Geological description of the tested North Sea materials

The examined sequence of strata in the North Sea region comprises diverse marine deposits formed during the postglacial, late glacial, and glacial periods, consisting of gravel, sand, silt, and clay, with lesser quantities of interglacial marine sediments.

The material under current investigation is characterized as moderately to densely compacted, olive-brown, slightly silty, gravelly, calcareous, uniformly graded, medium sand, containing shell fragments. This sand is differentiated from other soil types by the presence of mica, carboniferous fragments, and plant remains within it.

### 2.2. Ring shear apparatus

The Advanced ring shear apparatus (Bishop-like), illustrated in Fig. 1, functions as a robust tool for evaluating residual shear strengths at interfaces between soil-soil and soil-structure. Jardine et al. (2005) advocate for site-specific ring shear interface tests as an efficient approach to determine representative interface friction angles. These angles play a critical role in the detailed design of driven piles across diverse geological materials, including clays, sands, and even chalk. Liu et al. (2019) provide an overview of significant enhancements and modifications implemented in the Bishop ring shear apparatuses at both ICL and the NGI.

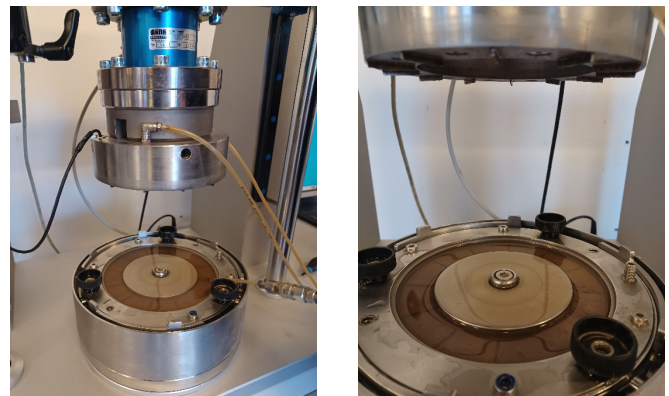


Figure 1. Soil interface configuration of advanced ring shear apparatus

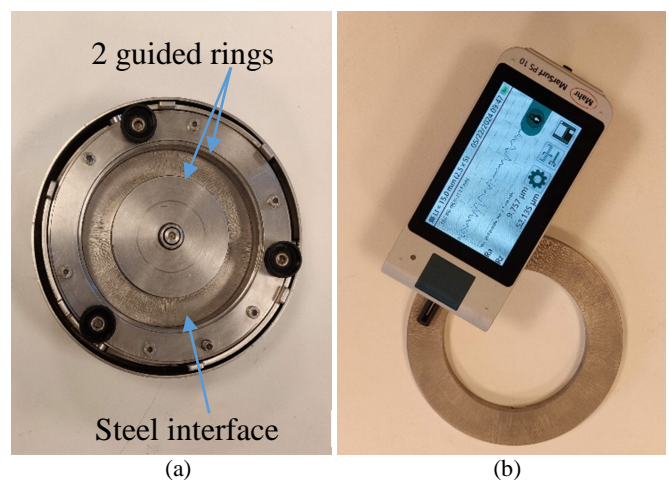
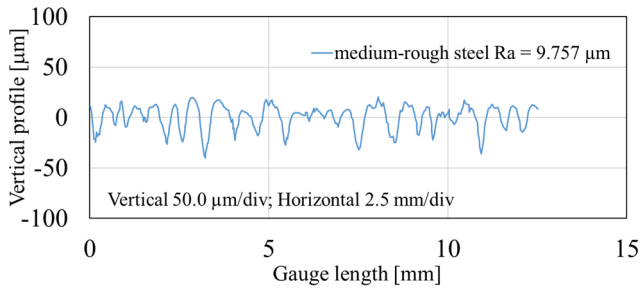


Figure 2. Soil interface configuration: (a) bottom ensemble of the ring shear apparatus (b) steel interface and the Mobile roughness measuring instrument MarSurf PS10



**Figure 3.** Example of the surface roughness profiles of medium-rough steel interface

The apparatus in Fig. 1 is capable of conducting tests on intact, reconstituted, or remoulded soils, accommodating soil-soil or soil-interface testing. The apparatus have two new test inserts compared to the Bishop ring shear, which have the option of rotating separately at different radial speeds, but are guided at the same time. The two guided rings as shown in Fig. 1 can move vertically and thus reduce static friction effects even with dilatancy. For soil-interface testing, configurations for lower interfaces is available.

The advanced ring shear apparatus have the following properties:

- (1) The complete ring shear system is made of stainless steel and includes upper and lower shear rings, porous ring plates with or without ribs, load pistons and water receivers for saturated conditions. Incorporation of electrical transducers for measuring displacements and loads.
- (2) Capability for torsional shearing at a wide range of rotation rates  $180^\circ - 0.00001^\circ/\text{min}$ , with normal and shear stresses up to 2 MPa. The shear ring sizes are 100 / 70 mm, 150 / 100 mm resembling Bromhead and Bishop device shear rings, respectively.
- (3) High-resolution data acquisition system with high-quality transducers for shear stress, normal stress, shear strain and axial strain with accuracy class 0.1 %.

### 2.3. Test procedures

Sandy soil specimens are prepared to achieve the desired initial dry density through the application of moist tamping techniques. The approach aligns with the guidelines proposed by Ladd (1978) that aim to mimic in-situ moisture levels and density conditions whenever possible. To ascertain the friction angles essential for designing axially loaded driven piles, engineers commonly employ the ICP procedures outlined by Jardine et al. (2005). These procedures, which can be adjusted to accommodate particular conditions or shearing histories, involve:

- (1) The steel interface roughness: A rough annular steel interface with an average roughness (Ra) of 10 µm was used. The average roughness, Ra, is defined as the arithmetic mean deviation of the

roughness profile. The interface roughness was measured before and after testing using a mobile roughness measuring instrument, the MarSurf PS10. Fig. 2 and Fig. 3 illustrate the MarSurf PS10 and the typical vertical profiles obtained from these measurements.

- (2) Installation and saturation of the specimen
- (3) Consolidation to a vertical effective stress equivalent to the initial in-situ free-field horizontal effective stress  $\sigma'_{r0}$ .
- (4) The upper ring is lifted in order to create a gap of 0.35 mm, under constant normal load. If the soil is squeezing under the ring, the gap is reduced and the vertical load re-adjusted. The shearing gap can be adjusted by screwing the knurled nuts as shown in Fig. 1.
- (5) Pre-shearing for 1 meter up to five times at fast rates (500 mm/min) to simulate pile driving. Each fast shear step followed by a pause of 10 minutes. Afterwards, any additional pore pressures are allowed to dissipate.
- (6) Consolidation to the radial effective stress  $\sigma'_{rc}$  anticipated at the pile shaft after the complete equalization of all effects of pile installation.
- (7) Slow shearing to 45 mm. This should be conducted at rates that ensure full drainage that may be assessed from the earlier consolidation stages. In general, the rate is calculated based on the end of primary consolidation, rate =  $45\text{mm} / t_f$ , where  $t_f = 13 t_c$ .  $t_c$  is the time to reach the end of primary consolidation and  $t_f$  is time to mobilise the maximum shear resistance of the specimen. The default rate for sand is 0.7 mm/min.

Jardine et al. (2005) introduced equations that describe the radial effective stresses ( $\sigma'_{r0}$  and  $\sigma'_{rc}$ ) applicable to tubular steel or concrete piles driven into silica sands.

For the fast-shearing phase: the radial effective stress  $\sigma'_{rc}$  estimated using the  $K_0$  value assessed from the OCR.

$$\sigma'_{r0} = K_0 \cdot \sigma'_{v0} \quad (1)$$

For slow shearing phase  $\sigma'_{rc}$ : considering the radial pressure on piles after dissipation of pore pressures using the formula proposed by Jardine et al. (2005), i.e.:

$$\sigma'_{rc} = 0.029 \cdot q_c \cdot (\sigma'_{v0} / P_a)^{0.13} (h / R^*)^{-0.38} \quad (2)$$

$$\tau_{rzf} = \sigma'_{rf} \cdot \tan \delta'_{ult} \quad (3)$$

In this context,  $\sigma'_{v0}$  and  $\sigma'_{r0}$  refer to the local free-field vertical and radial effective stress, respectively, while  $K_0$  represents the earth pressure coefficient at rest.  $\sigma'_{rc}$  denotes the radial effective stress post-installation and equalization, which is contingent upon  $\sigma'_{v0}$ , local cone penetration test (CPT) resistance  $q_c$ , relative depth to pile tip  $h$ , and the equivalent pile radius  $R^*$ . The equivalent pile radius is  $R^* = (R_{outer}^2 - R_{inner}^2)^{0.5}$  for open- or closed-ended tubular piles, where  $R_{outer}$  and  $R_{inner}$  are outer and

inner diameter of the pile, respectively.  $P_a$  represents the atmospheric pressure (101.3 kPa).  $\tau_{rf}$  and  $\sigma'_{rf}$  denote shear stress and effective radial stress at pile shafts at failure, respectively, and are related to the ultimate interface friction angle  $\delta'_{ult}$ . Distinct expressions are applicable to other pile cross-sections.

### 3. Test Results and Interpretation

Ring shear tests were conducted in order to obtain the interface friction angles ( $\delta'$ ) that govern the shear stress which can be mobilised on the shaft of a driven pile. For this purpose, 20 Ring shear tests were carried out on disturbed samples in accordance with ICP design methods for Driven piles in sand and clays: 2005 (Appendix A), Jardine et al. (2005). 19 tests were performed using the Bishop-size setup and one test was conducted using the Bromhead-size setup. A soil-steel interface was tested in all the samples conducted with Bishop-size setup. A soil-soil interface was tested in the Bromhead-size setup. The soil-steel interface is placed on the bottom of the specimens. All tests were performed utilising fast shear and slow shear phases, respectively. The derived interface friction angles ( $\delta'$ ) parameters are based on the slow shear phase.

A summary of the advanced ring shear test results of the current study is presented in Table 1 at the end of this article.

#### 3.1. Influence of normal effective stress ( $\sigma'_n$ )

Fig. 4 depicts the correlation between  $\delta'_{ult}$  and  $\sigma'_n$  observed in the set of tests where rapid conditioning shearing was followed by slow shearing. The results suggest a rise in  $\delta'_{ult}$  with increasing  $\sigma'_n$ .

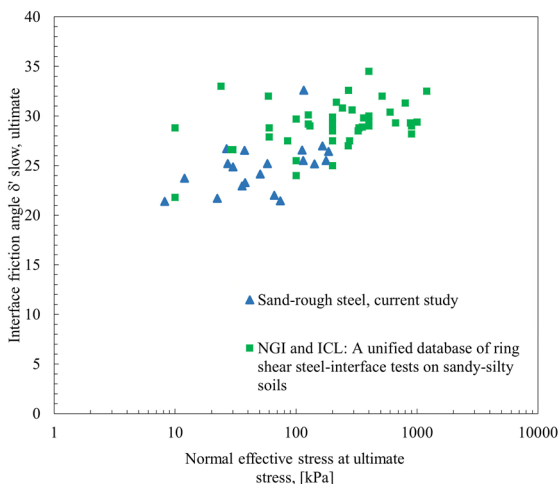


Figure 4. Relation between  $\delta'_{ultimate}$  and  $\sigma'_n$

The current study exhibited reduced scatter compared to the findings from the literature database. This disparity could arise from the use of different testing devices in the two studies, as well as variations in the geological properties of the tested material. Notably, the current study consistently yielded an interface friction angle with a discernible trend in tests conducted under low stresses

( $\sigma'_n < 50$  kPa), unlike those in the NGI and ICL unified database.

#### 3.2. Influence of $D_{50}$ on ultimate friction angles

The sand samples consistently displayed uniform initial particle size distributions, effectively summarized by the  $D_{50}$  value alone (cf. Table 1). Conversely, materials from shear zones post-testing often exhibited a wider array of grain sizes, with their  $D_{50}$  values sometimes failing to fully capture the significant influence of fines formed within these confined zones. This subsection presents plots correlating shear displacement at ultimate ( $\delta'_{ult}$ ) with initial  $D_{50}$  values.

Fig. 5 depicts the correlation between the  $\delta'_{ult}$ - $D_{50}$  relationship. Fig. 5 shows the  $\delta'_{ult}$ - $D_{50}$  data against the trends proposed from direct shear tests by Jardine et al. (1992), Ho et al. (2011), and Liu et al. (2019) from Bishop ring shear interface tests.

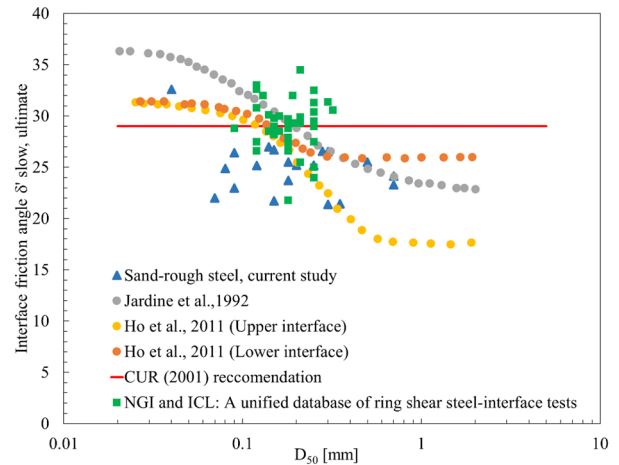


Figure 5. Comparison of  $\delta'_{ultimate}$  against  $D_{50}$

The authors'  $\delta'_{ult}$  values differ from the widely accepted  $\delta'_{ult} = 29^\circ$  value found in literature and the CUR (2001) recommendation, instead scattering around the patterns proposed by Ho et al. (2011) for the upper interface condition. These previous studies were performed using the ICP Bishop ring shear experiments on clean silica sands and non-plastic silts with stainless steel interfaces. The results displayed a reliance on normal effective stress  $\sigma'_n$  and demonstrated less significant fluctuations of  $\delta'_{ult}$  concerning  $D_{50}$  compared to experiments in literature, such as direct shear tests with smaller displacements and lacking preconditioning stages. The broader dispersion observed in the current study due to the wider variations in the specimens geology, normal effective stresses, soil consistency, fines content, and mineral composition.

#### 3.3. Influence of interface characteristics

In Fig. 6, the ultimate shear angles,  $\delta'_{ult}$ , are plotted against the normalized pre-test interface surface roughness ( $R_{CLA}/D_{50}$ ), following the correlation outlined



by Jardine et al. (1992) based on direct shear tests. Ring-shear interface tests conducted with relatively high  $R_{CLA}/D_{50}$  ratios show dispersion around the trend observed in Jardine et al. (1992). Initially, this trend shows a linear relationship between  $\tan(\delta'_{ult})$  and  $R_{CLA}/D_{50}$  until it reaches a plateau, indicating the critical state shearing resistance angle for soils.

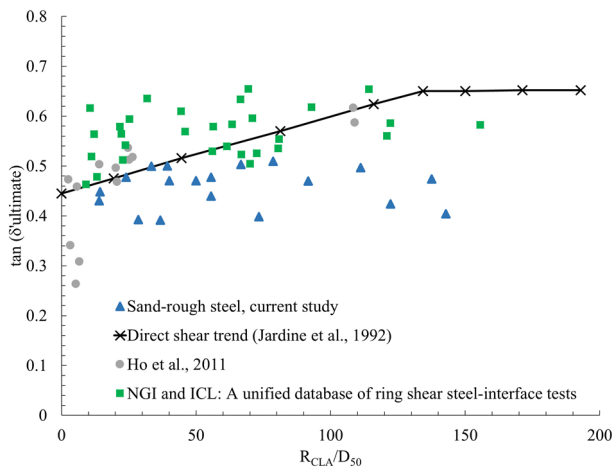


**Figure 6.** Correlation between  $\tan \delta'_{ult}$  and pre-test normalised roughness  $R_{CLA}/D_{50}$

Conversely, for lower ratios of  $R_{CLA}/D_{50}$ , the data illustrating the relationship between ring shear  $\tan(\delta'_{ult})$  and  $R_{CLA}/D_{50}$  consistently depict values below the trend observed in Jardine et al. (1992). In addition, the current data set showed a very good agreement with the results found by Ho et al. (2011). In contrast the NGI and ICL unified data set yielded values above the trend observed in Jardine et al. (1992), Ho et al. (2011) and the current study. The authors believe that the material mineralogy, grain size distribution and possibly the size of the gap between the interface and shearing ring contribute to changes in shear stress, ultimately leading to a reduction in the interface friction angle.

On the other hand, Liu (2018) proposed that the higher  $\delta'_{ult}$  values observed in ICP ring shear tests are attributed to the rapid conditioning shearing stages, which result in grain crushing and smoothing of the interface. Additionally, the less representative confining conditions in direct shear tests compared to those in the Bishop ring shear interface apparatus contribute to this phenomenon.

### 3.4. Relation between the $\delta'_{20mm}/\delta'_{ult}$ ratio and the normal effective stress ( $\sigma'_n$ )

Interface friction angles at a shear displacement of 20 mm ( $\delta'_{20mm}$ ) are commonly needed in pile design applications. Fig. 7 displays the relationship between the ratio  $\delta'_{20mm}/\delta'_{ult}$  and  $\sigma'_n$ , indicating that  $\delta'_{20mm}$  is approximately equal or higher than  $\delta'_{ult}$  by approximately 0.5 %. The ratio of  $\delta'_{20mm}$  to  $\delta'_{ult}$  in our study is lower than the correlation ratio found in literature. Herein, the ultimate interface friction angles ( $\delta'_{ult}$ ) were determined

at a shear displacement of approximately 45 mm, whereas the values in the available literature database were evaluated at around 50 mm of shear displacement. This indicates that as the shear displacement increases, the ratio between  $\delta'_{20mm}$  and  $\delta'_{ult}$  decreases due to the loss of material through the gap and possible further grain crushing.

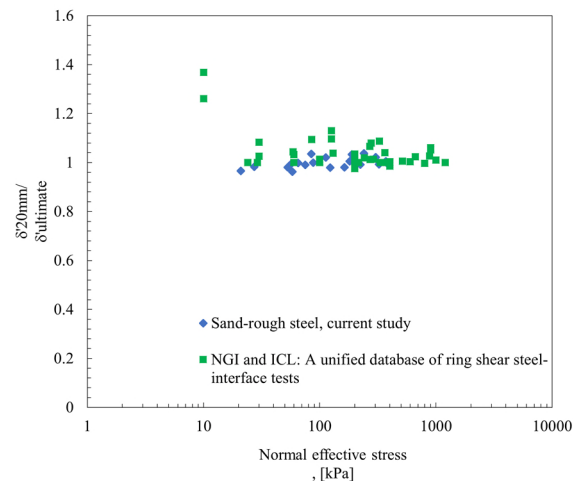


**Figure 7.** Relation between  $\delta'_{20mm}/\delta'_{ult}$  and  $\sigma'_n$

## 4. Conclusions

This paper presents a summary of 20 ring shear interface tests carried out at Geo on sandy-silty soils with a low proportion ( $\leq 25\%$ ) of non-plastic fines. The tests followed the ICP procedure proposed by Jardine et al. (2005), commonly used in designing driven piles for offshore wind-energy projects. The following conclusions are drawn from the results obtained:

The advanced ring shear apparatus (similar to Bishop's design) utilized in this study yielded interface friction angles that closely align with data found in the literature.

In general, the ring shear  $\delta'_{ult}$  values exhibited a clear dependence on normal stress ( $\sigma'_n$ ), increasing with  $\sigma'_n$  over a relatively high stress range ( $\sigma'_n > 50$  kPa).

The ultimate shear angles ( $\delta'_{ult}$ ) showed variability corresponding to  $D_{50}$  data similar to that described by Ho et al. (2011). However, factors such as interface roughness, and normal stress level significantly influenced these angles, resulting in noticeable variations.

Neither the simplistic assumption of  $\delta'_{ult} = 29^\circ$  nor reliance on direct shear interface tests proved as satisfactory as conducting site-specific ring shear tests.

Friction angles at peak shear stress ( $\delta'_{peak}$ ) were approximately 1 % higher than those at ultimate states ( $\delta'_{ult}$ ).

Although the existing database and correlations offer valuable assistance in initially estimating interface friction angles for design purposes, the authors recommend conducting interface testing customized to the particular soil and project conditions. This approach

guarantees precise determination of design parameters that accurately represent the in-situ soil conditions, interface properties, and effective stress levels

**Table 1.** Testing conditions and results and for the database

Borehole	R <sub>CLA</sub>	D <sub>50</sub>	Peak shear stress	Normal stress at peak stress	Shear stress at $\delta'_{slow, 20mm}$	Normal stress at $\delta'_{slow, 20mm}$	Ultimate shear stress	Ultimate normal stress	$\delta'_{slow, peak}$	$\delta'_{slow, 20mm}$	$\delta'_{slow, ultimate}$
-	mm	mm	kPa	kPa	kPa	kPa	kPa	kPa	°	°	°
002	11.1 ± 2.1	0.08	31	65	30	65	30	65	25.4	24.8	24.9
003	10.8 ± 1.6	0.25	28	58	26	58	27	58	25.5	24.3	25.2
013	10.9 ± 1.5	0.18	180	370	178	371	177	370	26.0	25.7	25.5
022	11.3 ± 1.7	0.14	170	324	163	323	165	324	27.7	26.8	27.0
024	Soil-soil	0.04	118	181	117	182	116	181	33.0	32.8	32.6
027	11.1 ± 2.01	0.09	38	85	37	85	36	85	24.2	23.8	23.0
027A	10.8 ± 1.5	0.7	52	112	51	112	50	113	25.0	24.6	24.2
029	10.9 ± 1.56	0.15	27	53	26	53	27	53	27.3	26.2	26.7
030	10.3 ± 1.8	0.09	190	373	185	373	186	374	27.0	26.4	26.4
039	10.8 ± 1.1	0.3	39	75	37	75	37	75	27.2	26.3	26.5
042	10.6 ± 1.3	0.35	80	189	77	189	74	189	23.1	22.1	21.4
050	10.6 ± 1.2	0.2	60	123	56	123	58	123	25.8	24.7	25.2
059	11 ± 1.9	0.15	26	56	22	56	22	56	25.3	21.5	21.7
062	11.6 ± 1.6	0.28	113	224	111	224	112	224	26.8	26.4	26.6
063	12.1 ± 1.7	0.5	123	238	119	240	115	240	27.3	26.5	25.5
066	11.3 ± 1.2	0.3	8	21	8	21	8	21	21.9	20.7	21.4
072	10.4 ± 1.7	0.07	66	164	65	164	66	164	22.1	21.6	22.0
084	11 ± 1.5	0.12	148	304	146	303	142	303	26.0	25.7	25.2
096	10.6 ± 1.5	0.18	12	27	12	27	12	27	23.7	23.3	23.7
100	9.8 ± 1.2	0.7	38	87	38	88	38	88	23.7	23.3	23.3

## Acknowledgements

We would like to thank SSE Renewables for granting permission to publish these data. Additionally, we acknowledge Geo for the time allocated to the preparation of this manuscript.

## References

Andersen, K. H., Puech, A. A. & Jardine, R. J. (2013) Cyclic resistant geotechnical design and parameter selection for offshore engineering and other applications. In 18<sup>th</sup> International Conference on Soil Mechanics and Geotechnical Engineering. (Al, D. E. (ed)) des Ponts, Paris, vol. 1.

Barmopoulos, I., Ho, T., Jardine, R. J. & Anh-Minh, N. (2010) The large displacement shear characteristics of granular media against concrete and steel interfaces. In Proceedings of the Research Symposium on Characterization and Behavior of Interfaces. (Frost, J. (ed)) IOS press, Atlanta, USA.

Bishop, A. W., Green, G. E., Garga, V. K., Andresen, A. & Brown, J. D. (1971) A new ring shear apparatus and its application to the measurement of residual strength. *Geotechnique* 21(4):273-328.

Bromhead, E. N. and Dixon, N. (1986) Field residual strength of London Clay and its correlation with laboratory measurements, especially ring-shear tests, *Geotechnique*, 36, No. 3, 449-452.

Coop, M., Sorensen, K., Freitas, T. B. & Georgoutsos, G. (2004) Particle breakage during shearing of a carbonate sand. *Geotechnique* 54(3):157-164.

CUR (2001). Bearing capacity of steel pipe piles, Report 2001-8. Gouda, the Netherlands: Centre for Civil Engineering Research and Codes.

Fearon, R. (1998) The behaviour of a structurally complex clay from an Italian landslide. PhD Thesis, City University, London.

Ho, T., Jardine, R. J. & Anh-Minh, N. (2011) Large-displacement interface shear between steel and granular media. *Geotechnique* 61(3):221.

Jardine, R. J., Lehane, B. M. & Everton, S. J. (1992) Friction coefficients for piles in sands and silts. In *Offshore Site Investigation and Foundation Behaviour*. (Ardu, D. A., et al (eds)) Society for Underwater Technology, Dordrecht, pp. 661-677.

Jardine, R. J. & Chow, F. C. (1996). New design methods for offshore piles. London: Marine Technology Directorate

Jardine, R. J., Chow, F. C., Overy, R. F. & Standing, J. R. (2005) ICP design methods for driven piles in sands and clays. London, Thomas Telford.

Ladd, R. (1978) Preparing test specimens using undercompaction. *Geotechnical Testing Journal*, 1(1): 16-23.

Liu, T. F. (2018) Advanced laboratory testing for offshore pile foundations under monotonic and cyclic loading, PhD thesis, Imperial College London.

Liu, T. F., Quinteros, V. S., Jardine, R.J., Carraro, J. A. H., and Robinson, J. A unified database of ring shear steel-interface

tests on sandy-silty soils. Submitted to ECSMGE, Reykjavik (2019)

Stark, T. D. & Vettel, J. Bromhead Ring Shear Test Procedure, *Geotechnical Testing Journal*. GTJODJ. Vol. 15. No.1, March 1992. pp. 24-32.

Stark, T. D. & Eid, H. T., 1992, Comparison of Field and Laboratory Residual Strengths, *Proceedings, ASCE Specialty Conference Stability and Performance of Slopes and Embankments-II*. University of California, Berkeley, CA, ASCE, New York.